Hot Tap Welding Model

Ravi Kedarasetti

1 Problem statement

Hot tapping[1](or pressure tapping) is the method of connecting to a "live" pipeline or tank containing a pressurized fluid, without removing the pipe or tank from service. When welding is used to add attachments to a pipeline during hot tapping, the heat transfer around the weld could me a major concern. If the unmelted portion of pipe wall beneath the weld is not thick enough, it might not withstand the pressure of the fluid. In some cases, the excess cooling provided by the flowing liquid could lead to cold cracking of the weld. Thermal models are often used to simulate the head transfer around the welds to estimate the safe operating ranges for heating rates to prevent burn through and cold cracking[2].

Consider a simplified, axisymmetric thermal model of hot taping process, where a sleeve is welded onto a live pipe carrying fluid. In this problem, a cylindrical stainless steel sleeve of thickness t_{sleeve} and length L_{sleeve} is welded onto a pipe of outer radius r_0, wall thickness of t_{wall} and a length of L_{wall}, with a small gap of thickness t_{gap} between the wall and the sleeve, as shown in figure 1. The cross section of the weld is assumed to be a right-angled isosceles triangle. The material in the whole model has a mass-density ρ, thermal conductivity κ and heat capacity c_p. During the welding process, heat $f(r, z, t)$ is supplied to the weld. The inner wall of the pipe is in contact with the fluid being transported at temperature u_p, while the outer wall of the entire geometry is surrounded by ambient atmosphere at temperature u_a The heat transfer coefficients at the inner and outer walls are h_p and h_a respectively. The surface of the walls facing the gap between the sleeve and the pipe, and the axial ends of the sleeve and the pipe are assumed to be insulated. The boundary conditions are depicted in figure 1. The parameters and their units are presented in table 1.

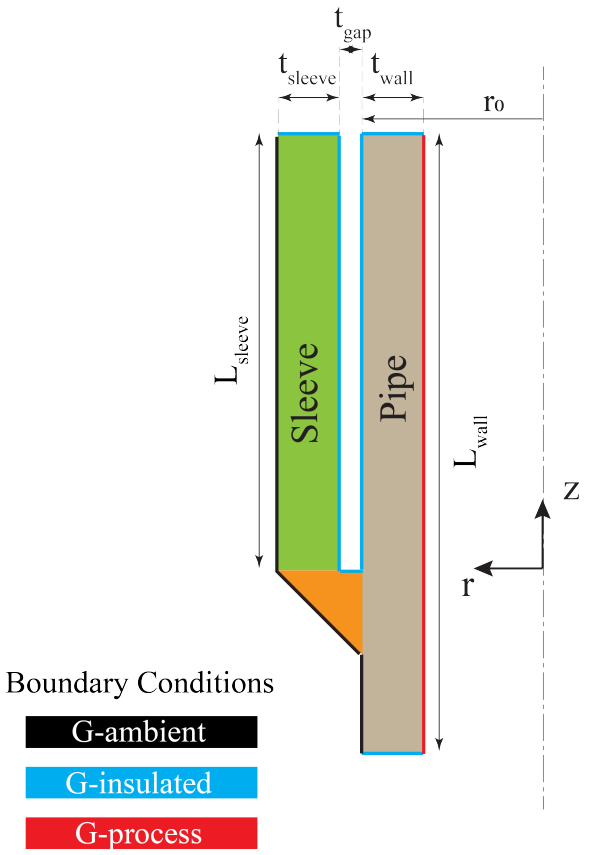

Figure 1: Axisymmetric model showing the pipe (brown), sleeve (green) and weld(orange) geometries and the boundary conditions

[1]TWI-Global. *Hot Tapping*. URL: `https://www.twi-global.com/technical-knowledge/faqs/faq-what-is-hot-tapping`.

[2]William A Bruce and Matthew A Boring. "Comparison of methods for predicting safe parameters for welding onto in-service pipelines". In: *International Pipeline Conference*. Vol. 42630. 2006.

Parameter	Value	Unit	Description
t_{sleeve}	0.188	in	Sleeve thickness
L_{sleeve}	$10 * t_{sleeve}$	in	Sleeve Length
t_{wall}	t_{sleeve}	in	Pipe wall thickness
L_{wall}	$1.5 * L_{sleeve}$	in	Pipe wall length
t_{gap}	0.02	in	Gap Thickness
t_{weld}	$t_{sleeve} + t_{gap}$	in	Weld height
ρ	0.284	lb/in^3	mass density
c_p	0.199	$BTU/lb - F$	heat capacity
κ	31.95	$BTU/ht - ft - F$	heat conductivity
u_a	70	F	Ambient temperature
h_a	9.0	$BTU/hr - ft^2 - F$	Heat transfer coefficient - ambient
u_p	325	F	Internal fluid temperature
h_p	48.0	$BTU/hr - ft^2 - F$	Heat transfer coefficient - Internal fluid
f_{max}	1350	$BTU/s - in^3$	maximum heat generated

Table 1: Model parameters

2 Formulation

2.1 Strong form

This model is based on the linear heat equation. The spatio-temporal evolution of temperature u is governed by equation 1, where Ω_s, Ω_p and Ω_w are the domains representing the sleeve, pipe and weld respectively. The timecourse of the heat source is defined in equation 2.

$$\rho c_p \frac{\partial u}{\partial t} = \kappa \nabla^2 u + f(r,z,t) \qquad in\ \Omega = \Omega_s \cup \Omega_p \cup \Omega_w \tag{1}$$

$$f(r,z,t) = \begin{cases} f_{max}(1 + \cos\frac{\pi}{5}(t+5)) & in\ \Omega_w \\ 0 & in\ \Omega_s \cup \Omega_p \end{cases} \tag{2}$$

The boundary conditions are given by equations 3-5, where Γ_a, Γ_i and Γ_p are the boundaries G-ambient, G-insulated and G-process, shown in figure 1.

$$on\ \Gamma_a \qquad -\kappa \frac{\partial u}{\partial n} = h_a(u - u_a) \tag{3}$$

$$on\ \Gamma_i \qquad -\kappa \frac{\partial u}{\partial n} = 0 \tag{4}$$

$$on\ \Gamma_p \qquad -\kappa \frac{\partial u}{\partial n} = h_p(u - u_p) \tag{5}$$

2.2 Weak form

For the weak formulation, we define the functional space V (equation 6), where $d = 2, 3$ is the number of spatial dimensions in the problem. Since there are no Dirichlet boundary conditions in this problem, the trail functions u and the test functions v are taken from the same space. The weak form is given by equation 7, where the bilinear and linear forms are defined by equations 8 and 9 respectively, where the volume and surface elements are represented by dx and ds respectively.

$$\mathcal{V} := \left\{ u \in L^2(\Omega) \mid \boldsymbol{\nabla} u \in L^2(\Omega)^d \right\} \tag{6}$$

$$find\ u \in \mathcal{V},\ s.t.\ \forall v \in \mathcal{V}, \qquad a(u,v) = L(v) \tag{7}$$

$$a(u,v) = \int_\Omega \rho c_p \frac{\partial u}{\partial t} v dx \int_\Omega \kappa \boldsymbol{\nabla} u \cdot \boldsymbol{\nabla} v\ dx + \int_{\Gamma_a} h_a uv\ ds + \int_{\Gamma_p} h_p uv\ ds \tag{8}$$

$$L(v) = \int_\Omega f(r,z,t) v\ dx + \int_{\Gamma_a} h_a u_a v\ ds + \int_{\Gamma_p} h_p u_p v\ ds \tag{9}$$

3 FEniCS implementation

The problem is implemented using an axisymmetric geometry in FEnics. First order Lagrange polynomials ($\mathcal{P}^1$) over a triangular mesh are used as the finite element functional space. The time integration is implemented using the backward Euler (implicit) method. The solution (u^{n+1}) for each time step (t^{n+1}) is calculated according to equations 10 to 12, where dt is the time step and the solution of the previous time step u^n is taken as a known variable.

$$find\ u^{n+1} \in \mathcal{P}^1,\ s.t.\ \forall v \in \mathcal{P}^1, \qquad a(u^{n+1},v) = L(v) \tag{10}$$

$$a(u^{n+1},v) = \int_\Omega \rho c_p u^{n+1} v dx \int_\Omega \kappa \boldsymbol{\nabla} u \cdot \boldsymbol{\nabla} v\ dt\ dx + \int_{\Gamma_a} h_a uv\ dt\ ds + \int_{\Gamma_p} h_p uv\ dt\ ds \tag{11}$$

$$L(v) = \int_\Omega f(r,z,t^{n+1}) v\ dt\ dx + \int_{\Gamma_a} h_a u_a v\ dt\ ds + \int_{\Gamma_p} h_p u_p v\ dt\ ds + \int_\Omega \rho c_p u^n v dx \tag{12}$$

The geometry is created using regular 2D shapes in the *mshr* module (*Rectangle* for the pipe and sleeve, and *Polygon* for the weld). Subdomains are created in the combined geometry for the three regions so that the mesh generated also has these subdomains. Three boundary subdomains are created to represent Γ_i, Γ_a and Γ_p.

This model is 2D axisymmetric,which means that the 2D geometry in the model represents the physical 3D shape. This is achieved by assuming that none of the variables in the model change in the circumferential direction and modifying the volume and surface integrals accordingly. The volume and surface integrals for any function have to be modified as specified in equations 13 and 14 respectively, where dX and dS are the area and line integrals in the 2D axisymmetric geometry. In FEniCS, this is implemented by multiplying each term by $2pix[0]$

$$\int_{\Omega_s} f dx = \int_{\Omega_s} g(2\pi r) dX \tag{13}$$

$$\int_{\Gamma_s} g ds = \int_{\Omega_s} g(2\pi r) dS \tag{14}$$

The code is available at

Note: In terms of spatial derivatives, the weak formulation of this problem only involves gradients of scalars. The components of gradient of scalars in the first two coordinates look identical for the r-z coordinates and x-y coordinates, and therefore the built-in grad function is used. For problems involving higher order derivatives and gradients of vectors, custom functions need to be written for calculating spatial derivatives in 2D axisymmetric coordinates.

3.1 Initial condition

The initial value of the temperature is calculated by solving the stationary problem, whose finite element form is given by equation 15.

$$find\ u^0 \in \mathcal{P}^1,\ s.t.\ \forall v \in \mathcal{P}^1, \qquad a(u^0, v) = L(v) \tag{15}$$

$$a(u^0, v) = \int_\Omega \kappa \boldsymbol{\nabla} u \cdot \boldsymbol{\nabla} v\ dx + \int_{\Gamma_a} h_a uv\ ds + \int_{\Gamma_p} h_p uv\ ds \tag{16}$$

$$L(v) = \int_{\Gamma_a} h_a u_a v\ ds + \int_{\Gamma_p} h_p u_p v\ ds \tag{17}$$

4 Results and observations

4.1 Overheating with proposed heating

The temperature profile in the model and the temporal evolution of the temperature at the midpoint of the weld facing the pipe and the sleeve are shown in figure 2. This model suggests that almost the entire length of the sleeve and the pipe melt during the welding process. Since all the material parameters closely match the properties of stainless steel, I conclude that the heating rate in the proposed problem is too high.

For the rest of the report, I used a maximum heating rate f_{max} of 270 $BTU/s - in^3$.

4.2 Heat affected zone

The results of the model with the modified cooling rate are shown in figure 3. The weld material heats up and reaches melting temperature within ? seconds. The weld pool starts forming at the pipe in ? seconds. The temperatures and the cooling rates at different points on the pipe are shown in figure 3B. Assuming a cutoff of $1475\,\mathrm{deg}\,F$ $(1075K)$[3], the width of the heat affected zone is ?in. These temperature profiles can be used as an input for a microstructure model to estimate the possibility of cold cracking.

5 Discussion

The simulation presented here has several limitations. It is based on a linear heat transfer model and does not simulate the latent heat of melting and solidification, the interface between the solid and fluid phases and the the formation of different metallurgical phases. The fluid flow in the pipes is not explicitly modeled and therefore the effect of the fluid flow on the cooling rate and the effect of heating on the fluid flow cannot be fully understood by this model. The heating of the weld element is assumed to be a volumetric heat term, while in reality welding is performed by passing a heating element over the weld zone. Finally, the assumptions of the geometry made in this model are not completely true-to-life, as the geometry of attachments to pipelines are not usually symmetric around the pipe's axis. Some of these limitations will be addressed here.

5.1 Fluid flow modeling

In this simulation, the heat transfer at the wall of the pipeline is modeled by means of a single constant h_p, which is the heat transfer coefficient of the fluid in the pipe. This kind of model is usually sufficient to understand the heat transfer in the pipe wall and the heat transfer coefficient can be changed based on the Nusselt number of the fluid flow in the pipe. There are several models available for the calculation of the Nusslet number for laminar and turbulent flows[4]. This lumped parameter model can be replaced by explicit models of fluid flow and heat transfer using the convection-diffusion equation. However, fluid flow simulations can be computationally expensive, especially in the turbulent flow regime and therefore the lumped parameter model used here should be preferred.

[3] Wentao Cheng et al. "Weld microstructure and hardness prediction for in-service hot-tap welds". In: *International Pipeline Conference*. Vol. 41766. 2004.

[4] Endre Nagy. *Basic equations of mass transport through a membrane layer*. Elsevier, 2018.

Fluid flow and heat transfer in gas-fluid mixtures can be very complicated depending on the gas/fluid ratio and the inclination of the pipeline, as gravity plays an important role in the separation of the phases[5]. These models can also be computationally expensive and can be replaced by heat transfer coefficients calculated based on experimental data for different gas/fluid ratios and pipe inclinations[6,7,8].

5.2 3D modeling

The current model is 2D axisymmetric and assumes that a cylindrical attachment is welded over the entire circumference of the pipe. As long as an attachment is placed over the entire circumference of the pipe, we can use an axisymmetric model, where the attachments geometry is replaced with a cylindrical geometry of equivalent thermal resistance. The heat flow through the sleeve/attachment in this configuration is through its contact with the weld and through its outer walls facing the atmosphere. Based on the Biot number at these two faces, a non-axisymmetric geometry can be replaced by an equivalent cylindrical geometry[9]. For attachments that do not cover the entire circumference of the pipe, like branching pipes, 3D models are more suitable[10].

5.3 Heat source modeling

In this problem, the welding heat source is modeled as a spatially uniform time-dependent power density in the entire weld area. A more widely accepted method for modeling the heat source for MIG welding assumes a double-ellipsoid geometry for the power density[11]. In this method, the power density is given by the sum of two Gaussian terms given by equation 18 in the direction of the moving weld and 19 in the trailing direction. In equations 18 and 19, the weld is moving in the z direction, with the origin at the base of the weld. Q is the power source density and a, b, c_f and c_r define the spread of the weld power in x, y and z directions. The relative power distribution in the forward and trailing directions of the weld are given by f_f and f_r respectively. The speed motion of the welding source is given by v (equation 20). This heat source model is often used in simulations performed in the frame of reference moving with the welding source, and applied to a cross section of the geometry perpendicular to the welding source motion[12]. In this case, ζ would be a function of time only. However, to make accurate predictions of the effect of parameters[13], and to simulating cases of multipass welding[14], 3D models are preferred.

$$q(x,y,z,t) = \frac{6\sqrt{3}f_f Q}{abc\pi^{\frac{3}{2}}} e^{-3x^2/a^2} e^{-3y^2/a^2} e^{-3\zeta^2/c_f^2} \tag{18}$$

$$q(x,y,z,t) = \frac{6\sqrt{3}f_b Q}{abc\pi^{\frac{3}{2}}} e^{-3x^2/a^2} e^{-3y^2/a^2} e^{-3\zeta^2/c_r^2} \tag{19}$$

$$\zeta = z + v(\tau - t) \tag{20}$$

[5]Hong-Quan Zhang et al. "Unified model of heat transfer in gas-liquid pipe flow". In: *SPE Production & Operations* 21.01 (2006).

[6]Dongwoo Kim et al. "Comparison of 20 two-phase heat transfer correlations with seven sets of experimental data, including flow pattern and tube inclination effects". In: *Heat Transfer Engineering* 20.1 (1999).

[7]Dongwoo Kim and Afshin J Ghajar. "Heat transfer measurements and correlations for air–water flow of different flow patterns in a horizontal pipe". In: *Experimental Thermal and Fluid Science* 25.8 (2002).

[8]Afshin J Ghajar and Clement C Tang. "Importance of non-boiling two-phase flow heat transfer in pipes for industrial applications". In: *Heat Transfer Engineering* 31.9 (2010).

[9]Timothy S Fisher et al. "Efficient heat transfer approximation for the chip-on-substrate problem". In: (1996).

[10]XiaoLong Xue et al. "Numerical simulation of in-service welding of a pressurized pipeline". In: (2007).

[11]John Goldak, Aditya Chakravarti, and Malcolm Bibby. "A new finite element model for welding heat sources". In: *Metallurgical transactions B* 15.2 (1984).

[12]L-E Lindgren. "Numerical modelling of welding". In: *Computer methods in applied mechanics and engineering* 195.48-49 (2006).

[13]D Gery, H Long, and P Maropoulos. "Effects of welding speed, energy input and heat source distribution on temperature variations in butt joint welding". In: *Journal of materials processing technology* 167.2-3 (2005).

[14]Dean Deng and Hidekazu Murakawa. "Numerical simulation of temperature field and residual stress in multi-pass welds in stainless steel pipe and comparison with experimental measurements". In: *Computational materials science* 37.3 (2006).

5.4 Microstructure modeling

Computational thermodynamic and kinetic calculations are used to estimate the distribution of various microstructural phases such as martensite and ferrite, and the hardness of the weld and the heat affected zone. The thermodynamic models are used to calculate the free energy of the mixture as a function of the temperature and the phase composition. The free energy minimization is used to calculate the equilibrium compositions. The equilibrium reactions and the kinetics of the reactions, along with the temperature history from heat simulations are used to predict the microstructure in the heat affected zone after cooling. Some models perform heat transfer calculations separately to predict the temperatures history and use it as an input for microstructure prediction[15,16,17], while other models couple the heat transfer and microstructural calculations[18,19,20].

5.5 Model extensions

5.6 Possible improvement of the model

[15] Cheng et al., see n. 3.

[16] V Mazurovsky et al. "The phenomenological model of non-equilibrium crystallization and strengthening-phase-formation processes in the weld". In: *Proceedings of the Bi-National Israeli-Russian Workshop, Jerusalem, Israel*. 2003.

[17] SS Babu, S David, and MA Quintana. "Modeling microstructure development in self-shielded flux cored arc welds". In: *WELDING JOURNAL-NEW YORK*- 80.4 (2001).

[18] C Henwood et al. "Coupled transient heat transfer—microstructure weld computations (Part B)". in: *Acta Metallurgica* 36.11 (1988).

[19] DF Watt et al. "An algorithm for modelling microstructural development in weld heat-affected zones (part a) reaction kinetics". In: *Acta Metallurgica* 36.11 (1988).

[20] M Victor Li et al. "A computational model for the prediction of steel hardenability". In: *Metallurgical and Materials transactions B* 29.3 (1998).